Response of a Tubular Heterogeneous Catalytic Reactor to a Step Increase in Flow Rate

CARL G. LEHR, SERGEI YURCHAK, and ROBERT L. KABEL

The Pennsylvania State University, University Park, Pennsylvania

The vapor phase dehydration of ethanol to diethyl ether, as catalyzed by ion exchange resin, has been studied experimentally and theoretically for the transient state period following a step increase in flow rate. A mathematical model is developed to account quantitatively for the effects of adsorption and surface reaction on the product distribution in the effluent of a tubular reactor. The solution of the model is in good agreement with the experimentally observed behavior.

A detailed understanding of the characteristics of chemical reactors during unsteady state operating conditions is becoming more important as automation within the chemical industry increases. The design of a process control system requires a mathematical model that properly accounts for the dynamic behavior of the reaction system. It is the purpose of this research to develop such a model for a tubular heterogeneous catalytic reactor and to demonstrate its capability by experiment.

The area of reactor dynamics has received extensive attention, both experimentally and especially theoretically in the past decade. Perspective in the field can be gained by studying some of the several good review papers (*3*, *5*, *9*, *13*). Two recent papers have contributed much to the understanding of the dynamic behavior of fixed-bed reaction systems. Crider and Foss (*4*) investigated, by means of mathematical models, the effects of "the thermal capacity of the packing, the resistance to heat flow between the packing and the fluid, the coupling of temperature and concentration through the rate of chemical reaction, axial fluid mixing, radial fluid mixing, and the loss of heat at the wall" on transients resulting from step changes in temperature or concentration of the feed. Although their reactor was packed with solid, the reaction was taken to be second-order irreversible and homogeneous. In a similar way, McGuire and Lapidus (*11*) investigated heat and mass transfer effects resulting from axial and radial gradients in the interparticle field and gradients plus reaction in the intraparticle field for a tubular reactor filled with a porous catalyst. For their model, they took the reaction to be first order and irreversible. It will be shown that consideration of a heterogeneous catalytic reaction system with appreciable adsorption adds another dimension to this problem. Since many processes of industrial importance fall in this category, the following development becomes of real practical interest.

The reaction system selected for study is the vapor phase dehydration of ethyl alcohol to diethyl ether as catalyzed by a cation exchange resin in the acid form:

$$2\,C_2H_5OH = (C_2H_5)_2O + H_2O \qquad (1)$$

This system was studied extensively by Kabel and Johanson (*6*, *7*) in an effort to experimentally assess the reasonableness and utility of the Langmuir-Hinshelwood model of heterogeneous catalysis. Kinetic data were well correlated by the Langmuir-Hinshelwood model and the surface reaction was found to be the rate controlling step. The Langmuir equilibrium adsorption constants in the kinetically determined rate equation were compared with the corresponding constants determined directly from pure component studies in a static adsorption system. The order of magnitude agreement between the constants for the three reacting components by these independent methods was taken as an indication that the Langmuir-Hinshelwood model accounts, in a reasonable way, for the adsorption effects for this particular catalytic reacting system. The work reported by Kabel and Johanson (*7*)

Carl G. Lehr is with the Xerox Corporation, Rochester, New York and Sergei Yurchak is at the University of Wisconsin, Madison, Wisconsin.

was entirely concerned with steady state. This paper deals with the transient response of the same system to a step change in flow rate.

STATEMENT OF PROBLEM

The problem was essentially five fold: (a) to obtain an expression for the rate of the catalytic reaction as a function of the catalyst surface coverage with ethanol, ether, and water, (b) to derive unsteady state material balance equations for ethanol, ether, and water, (c) to experimentally determine and/or theoretically account for the transient adsorption rate characteristics for the three reacting components, (d) to solve the unsteady state material balance equations simultaneously with the transient adsorption rate functions and the rate expression for the surface reaction, and (e) to experimentally determine the reactor response to a step change in flow rate for comparison to the corresponding response predicted mathematically.

TRANSIENT KINETIC STUDIES

In order to qualitatively understand which parameters are significant during the transient state period and to provide a sound basis for evaluation of the results of the mathematical model solution, it is necessary to have available actual reactor response data.

The first experimentally determined response to a step increase in ethanol flow rate was obtained by Kabel (*6*) at 105°C. and 1 atm. The experimental equipment and procedure are the same as reported by Kabel and Johanson (*7*) for the steady state studies with one exception. It was necessary to calibrate the gas chromatograph for water analysis as well as for ethanol and ethyl ether. The lack of refinement in the water calibration and the fact that this work was performed early in the overall experimental program mean that the data obtained are of less accuracy than the steady state data presented by Kabel and Johanson. Nevertheless the data, shown in Figure 1, point up well the salient features of the transient behavior.

Initially the reactor is at steady state corresponding to a pure liquid ethanol flow rate of 0.05 cc./min. The partial pressures of ether and water at the reactor outlet are 0.318 atm. and equal as they must be from the stoichiometry of the reaction. At zero time the flow rate of ethanol is immediately increased to its final value of 0.46 cc./min. After about 200 min. the reactor is again at steady state, with effluent partial pressures of ether and water equal to 0.042 atm. The obvious points to note at this time are: (a) the curves for ether and water partial pressures as functions of time are separated during the transient period, and (b) at fifty minutes into the transient period, the partial pressure of ether passes through a minimum.

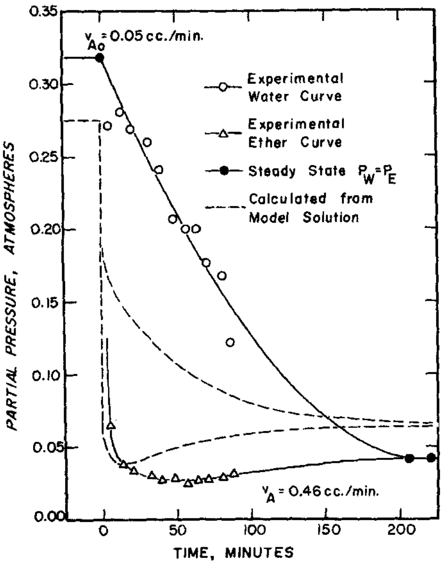

Fig. 1. Transient response of system to step increase in flow rate at 105°C. and 1.0 atm. total pressure.

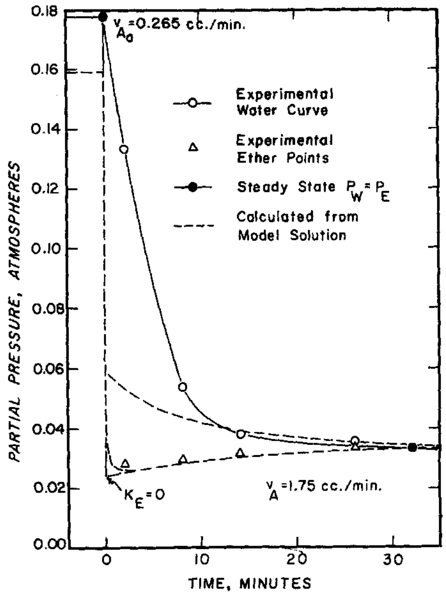

Fig. 2. Transient response of system to step increase in flow rate at 120°C. and 0.956 atm. total pressure.

During the course of the theoretical analysis an additional similar transient experiment was carried out at 120°C. and 0.956 atm. This temperature was selected because of the much better defined kinetics of the ethanol dehydration reaction. The apparatus used in this experiment followed along the lines of that reported by Kabel and Johanson. The method of product sampling and chromatographic analysis was considerably refined. Immediately following the reactor was a heated tube which lead to a gas sampling valve directly connected to a gas chromatograph. This arrangement eliminated sampling difficulties and appreciably improved ease and accuracy of analysis. A chromatographic column packing of polyethylene glycol on powdered Teflon allowed more accurate calibration and analysis for water than Kabel achieved with the same substrate on a diatomaceous earth support. The catalyst was Dowex 50, X-8, 20-50 mesh cation exchange resin (a sulfonated copolymer of styrene and divinylbenzene) in the hydrogen ion form. It has an exchange capacity of 0.0054 ± 0.0003 equivalents per gram of bone dry catalyst.* The catalyst sample used in this study was supplied by the same manufacturer and said to be of the same characteristics as that used by Kabel (*6*) in his studies. However the batches were produced several years apart and could conceivably result in slightly differing characteristics. In both experiments the partial pressure of ethanol may be obtained by subtracting the partial pressures of ether and water from the appropriate total pressure. Experimental equipment and procedure as well as further information on other aspects of this research are treated in detail elsewhere (*10*, *12*).

The results of this experiment are shown on Figure 2

---

* The catalyst was considered to be bone dry when no further material desorbed under evacuation at the temperature of interest.

in a manner analogous to Figure 1. At the lower flow rate of 0.265 cc./min. the steady state partial pressures of water and ether are identical at 0.178 atm. The final steady state at the higher flow rate of 1.75 cc./min. is reached in 32 min. with ether and water partial pressures equal to 0.033 atm. Again the separation of curves is noted, but in this case the minimum in the ether curve occurs near the beginning of the transient period. Unfortunately the minimum is not precisely located because the time required for analysis precluded more frequent sampling. These observations and others will be treated more fully in the next section of the paper.

THEORETICAL INTERPRETATION

Before one attempts to explain qualitatively or quantitatively the effects presented in the previous section it is necessary to establish a number of points concerning the reaction system. It has been demonstrated that under the conditions of interest, side reactions do not occur (*7*, *12*).

MASS TRANSFER EFFECTS

It was shown (*7*) that the following mass transfer effects are not significant under steady state conditions: (a) diffusional resistance within the catalyst pores, (b) concentration gradients between the catalyst surface and the bulk fluid, and (c) longitudinal and radial concentration gradients leading to backmixing in the tubular packed-bed reactor. Further studies by Yamas (*14*) confirmed Kabel's estimates on the backmixing effect by showing that it amounts to only 0.1% deviation in conversion from that calculated assuming plug flow.

Since mass transfer effects are negligible at steady state, one can limit consideration to the adsorption and surface reaction processes. The surface reaction was found to be the rate limiting step and thus the adsorption processes must be appreciably faster. In fact they are assumed to achieve equilibrium in the derivation of the steady state rate equation. The steady state mass transfer studies show only that mass transfer effects must be appreciably more rapid than the surface reaction. But mass transfer effects may not be negligible in comparison to the adsorption processes which are not at equilibrium during the transient state. For the purposes of this study however, since there is no information to the contrary, mass transfer effects are taken to be negligible for the transient case as well.

ADSORPTION AND REACTION RATE EQUATIONS

Following the usual Langmuir-Hinshelwood model, as systematized by Hougen and Watson, the following equations represent the adsorption-desorption processes and the surface reaction.

$$A + s = As \qquad (2)$$

$$2\,As = Ws + Es \qquad (3)$$

$$Ws = W + s \qquad (4)$$

$$Es = E + s \qquad (5)$$

Here A, E, and W refer to alcohol, ether, and water respectively, and *s* represents a site for activated adsorption.

For this postulated reaction path, which is in agreement with the results of Kabel and Johanson (*7*), rate equations for the four processes can be written

$$\rho_A = \kappa_A P_A \theta_V - \kappa_{-A}\theta_A \qquad (6)$$

$$r_A = k_A \theta_A^2 - k_{-A}\theta_W\theta_E \qquad (7)$$

$$\rho_W = \kappa_W P_W \theta_V - \kappa_{-W}\theta_W \qquad (8)$$

$$\rho_E = \kappa_E P_E \theta_V - \kappa_{-E}\theta_E \qquad (9)$$

In these equations and the work that follows, traditional symbols are used for surface reaction rate and rate coefficients. Corresponding Greek letters are used for the corresponding adsorption rate parameters. Standard notation will continue to be used for adsorption equilibrium constants. Since the Langmuir theory of activated adsorption is invoked here, the tacit assumption is made that adsorption proceeds only to the extent of a monolayer. This makes it possible to express the catalyst surface concentration in terms of the fractional surface coverage, θ. Thus $\theta_V = 1 - \theta_A - \theta_E - \theta_W$.

For the case of steady state operation, Kabel and Johanson showed the surface reaction to be the rate controlling step. By the equilibrium adsorption simplification and the usual manipulations the steady state rate equation is obtained:

$$r_A = \frac{k_A K_A^2[P_A^2 - (P_W P_E/K_{eq})]}{(1 + K_A P_A + K_W P_W + K_E P_E)^2} \qquad (10)$$

where $K_A = \kappa_A/\kappa_{-A}$, $K_W = \kappa_W/\kappa_{-W}$, and $K_E = \kappa_E/\kappa_{-E}$. The thermodynamic equilibrium constant is independently known (*8*) and is given by $K_{eq} = K_A^2 K/K_W K_E$, where $K = k_A/k_{-A}$.

Note that the assumption that the three adsorption processes are in equilibrium at the steady state is equivalent to the mathematical expression $\rho_A = \rho_E = \rho_W = 0$. In reality, at steady state, the adsorption rates must correspond to the reaction rate in the following way, $r_A = \rho_A = -2\rho_W = -2\rho_E$. However the use of this relationship in the derivation of a Langmuir-Hinshelwood type rate equation introduces three additional constants and a complexity which is not justified by the additional rigor.

During the transient state it cannot be assumed that the adsorption processes are in equilibrium because none of the processes on the reaction path are controlling. It is possible to develop a single expression for the rate of reaction, r_A, in terms of partial pressures and adsorption rates which applies during the transient period. This involves eliminating the four θ terms from Equations (6 to 9), but this yields an unwieldly expression which is much less convenient to use in computation than the equations it replaces.

QUALITATIVE EXPLANATION OF TRANSIENT RESULTS

In presenting Figures 1 and 2 it was noted that the ether and water did not appear in the same concentrations at the reactor outlet during the transient period and that the ether concentration fell significantly below its final steady state value. It can also be seen that the transient period in Figure 1 was much longer than in Figure 2. These points require some intuitive explanation and understanding before proceeding to the quantitative treatment of the phenomena.

Separation of Curves

From the stoichiometry of the reaction, Equation (1), it is seen that the chemical reaction must produce water and ether in equimolar amounts. Thus the presence of more water than ether in the vapor must be due to an additional source within the reactor. This source is the catalyst which is a strong adsorber of water.

It is a well known phenomenon that the amount of adsorbate in equilibrium with a vapor is proportional to the pressure of the vapor. Since the partial pressure of water at the initial steady state (low flow rate and large residence time) is greater than it will be at the final steady state (high flow rate and low residence time), it follows that θ_W is initially greater than θ_W at the new steady state. Thus there is more water on the catalyst initially than finally. During the transient period this excess water must be desorbed, and the number of moles of water in the vapor phase increases beyond that supplied by the chemical reaction. Ether is not adsorbed to such an extent (7), so it is produced mainly by the chemical reaction.

Ethanol, like water, is strongly adsorbed. Although its behavior is not shown on the Figures, it can be reasoned. Upon an increase in flow rate, the reduced residence time should yield an increased concentration of ethanol in the vapor and on the catalyst. Because additional ethanol must be adsorbed, ethanol will require some time to achieve the high value of concentration appropriate to the new steady state.

Ether Minimum Point

The minimum point in the ether partial pressure versus time curve occurs at approximately fifty minutes on Figure 1 and much sooner on Figure 2. It is easier to visualize what takes place if the minimum is instantaneous and then extend the discussion to account for the displaced minima.

Since the main production of ether comes from the chemical reaction, it is reasonable to state that the dependence of the partial pressure of ether on time at constant position in the reactor will follow the dependence of reaction rate on time at the same position. A minimum in the P_E vs. t curve is consequently synonymous to a minimum in the r_A vs. t behavior.

That a minimum in the reaction rate is to be expected under the conditions of these studies can be seen from Equation (7). The presence of a large amount of alcohol on the catalyst enhances the reaction whereas a large amount of water suppresses it. It was shown earlier that there is more water on the catalyst at the low flow rate (initial condition) than at the high flow rate (final steady state). Correspondingly the catalyst is poorer in alcohol initially than finally. These two effects, excess water and insufficient ethanol, reinforce each other in suppressing the rate of reaction. In fact this condition is most severe just after the flow rate adjustment. Thus the minimum rate occurs at the beginning of the transient period and the minimum ether concentration should occur at that point too if ether is not adsorbed. The ether data of Figure 2 approximate this situation. An identical minimum in the production of water must also occur. However there is no minimum point in the P_W vs. t curves of Figures 1 and 2 because the desorption of water masks the effects of the minimum rate of reaction.

Explanation of the more pronounced delayed minimum in the ether curve of Figure 1 can be obtained by consideration of differences in operating conditions between the runs. The data of Figure 1 were obtained at a temperature of 105°C. and the data of Figure 2 at 120°C. This temperature difference could account for a difference in the amount of ether initially adsorbed. At 120°C. ether adsorption has been shown to be very slight (7). At 105°C., however, small but more significant amounts of ether may be adsorbed. This point was not explored in the steady state work (7). Upon an increase in the flow rate, desorption of this ether partially masks the effect of the minimum rate but not enough to obscure the entire effect.

Length of the Transient Period

At 120°C. the transient period is seen to be much shorter than at 105°C. There are three major reasons for this. Most prominent is that the higher temperature accelerates the rate processes which will return the system to steady state. Second, the spread between the two steady state conversion levels is greater in the low temperature case. This means that a much greater departure of the initial catalyst conditions from the final steady state must be overcome. Third the new flow rate in the high temperature case is much higher than the new flow rate in the low temperature case. Other conditions being the same, a large space velocity will bring about a new steady state more rapidly than a small one. This fact is readily seen from experimental work in which the flow rate is reduced, rather than increased, to begin the transient.

UNSTEADY STATE MATERIAL BALANCES

In the determination of product concentrations at the outlet of a tubular reactor, one must integrate the equation which results from a material balance on a differential volume of the reactor. At steady state the stoichiometry of the reaction and a rate equation such as Equation (10) may be combined with the differential material balance to reduce the resulting differential equation to a single dependent variable, conversion, and a single independent variable, reactor volume.

In the transient case the adsorption effects preclude the use of stoichiometry to relate the reactant concentrations to one another. Thus independent material balance equations must be written over the differential element for each of the reaction components. The resulting equations must then be solved simultaneously.

The differential volume in the present work is taken to be a circular disk of differential thickness, dZ, and cross section equal to that of the tubular reactor. The material balances are written by considering the processes which tend to enrich and deplete the vapor of the differential element upon a step increase in flow rate. Ethanol will be brought into the volume by flow and will be removed by flow and chemical reaction.[†] Upon an increase in flow rate it will also be removed from the vapor by adsorption as explained earlier. The derivation below applies to ethanol with all terms having units of moles of ethanol per minute:

$$\text{Input by flow} = \frac{UA\rho_M P_A}{P}$$

$$\text{Output by flow} = \frac{A\rho_M}{P}\left[P_A + \frac{\partial P_A}{\partial Z}dZ\right] \left[U + \frac{\partial U}{\partial Z}dZ\right]$$

$$\text{Output by chemical reaction} = r_A \rho_c A dZ$$

$$\text{Output by adsorption} = (\kappa_A P_A \theta_V - \kappa_{-A}\theta_A)\rho_c A dZ$$

$$\text{Accumulation} = \frac{\rho_M \epsilon A}{P}\left[\frac{\partial P_A}{\partial t}\right]dZ$$

By setting input minus output equal to accumulation, cancelling terms, dividing by $\rho_c A dZ$, and noting that $\rho_M = P/RT$ yields the following equation:

$$-\frac{1}{\rho_c RT}\left(P_A\frac{\partial U}{\partial Z} + U\frac{\partial P_A}{\partial Z}\right) - r_A$$

[†] Actually ethanol is removed from the vapor only by adsorption. It is converted on the catalyst to ether and water which are returned to the vapor by desorption. Ideally this sequence of events should be accounted for by simultaneous material balances on the vapor and adsorbed phases. However the use of Equation (10) to correlate reaction rate data has yielded values for K_A, K_E, and K_W which already empirically allow for the amounts of adsorption and desorption which must accompany the surface reaction process. Thus in this derivation that portion of the adsorption processes must be ignored and the ethanol depletion by reaction may be considered as a vapor phase process.

$$-(\kappa_A P_A \theta_V - \kappa_{-A}\theta_A) = \frac{\epsilon}{\rho_c RT}\left(\frac{\partial P_A}{\partial t}\right) \tag{11}$$

Variations in superficial velocity through the reactor can be caused by changes in the temperature, pressure, reactor cross section, and total molar flow rate. The reactor was of constant cross section and was very nearly isothermal, and displaying deviations of less than 0.5°C. from the respective control points. The pressure drop through the reactor was less than 0.05% of the total pressure and the variations in the ambient pressure over the period of a run were negligible. An expression for the velocity gradient, $\partial U/\partial Z$, can be obtained from a total material balance on the same differential volume of the isothermal isobaric reactor. When the resulting expression is substituted into Equation (11) we obtain

$$-\frac{U}{\rho_c RT}\frac{\partial P_A}{\partial Z} - \frac{r_A \delta P_A}{P} + \frac{(\rho_A + \rho_E + \rho_W)P_A}{P} - r_A - (\kappa_A P_A \theta_V - \kappa_{-A}\theta_A) = \frac{\epsilon}{\rho_c RT}\left(\frac{\partial P_A}{\partial t}\right) \tag{12}$$

As can be seen from Equation (1) the reaction itself will produce no change in the total molar flow rate (that is: $\delta = 0$). On the other hand the three adsorption processes could result in a net depletion or augmentation of the flowing vapor. In this reaction system, ethyl ether is not strongly adsorbed and the desorption of water tends to compensate for the adsorption of ethanol (that is: $\rho_E \cong 0$, $\rho_A \cong -\rho_W$). Yurchak (*15*) showed by approximate calculations that the total surface coverage remains fairly constant during the transient state. Thus the change in velocity through the reactor will be small, especially in comparison with the new imposed velocity which is relatively high. Thus for the problem considered in this paper the velocity may be taken to be constant during the transient period. With $\partial U/\partial Z = 0$, Equations (11) and (12) become

$$-\frac{U}{\rho_c RT}\frac{\partial P_A}{\partial Z} - r_A - (\kappa_A P_A \theta_V - \kappa_{-A}\theta_A) = \frac{\epsilon}{\rho_c RT}\frac{\partial P_A}{\partial t} \tag{13}$$

The boundary conditions for Equation (13) are

$$P_A(Z, 0) = f(Z) \tag{14}$$

$$P_A(0, t) = P \tag{15}$$

$$P_A(Z, t) \rightarrow M, M > 0 \text{ at } Z = L \text{ as } t \rightarrow \infty \tag{16}$$

Condition (14) is the initial steady state distribution of P_A throughout the length of the reactor. Condition (15) states that the feed is pure ethanol. Condition (16) demonstrates the necessity for convergence of Equation (13), that is, it requires a new steady state to be established to end the transient period. The function, $f(Z)$ can be determined from the steady state solution of Equation (13).

Similarly the corresponding equations for water and ether are

$$-\frac{U}{\rho_c RT}\frac{\partial P_W}{\partial Z} + r_W + (\kappa_{-W}\theta_W - \kappa_W P_W \theta_V) = \frac{\epsilon}{\rho_c RT}\frac{\partial P_W}{\partial t} \tag{17}$$

$$-\frac{U}{\rho_c RT}\frac{\partial P_E}{\partial Z} + r_E + (\kappa_{-E}\theta_E - \kappa_E P_E \theta_V) = \frac{\epsilon}{\rho_c RT}\frac{\partial P_E}{\partial t} \tag{18}$$

$$P_W(Z, 0) = P_E(Z, 0) = g(Z) \tag{19}$$

$$P_W(0, t) = P_E(0, t) = 0 \tag{20}$$

$$P_W(Z, t) \rightarrow N, N > 0 \text{ at } Z = L \text{ as } t \rightarrow \infty \tag{21}$$

$$P_E(Z, t) \rightarrow N, N > 0 \text{ at } Z = L \text{ as } t \rightarrow \infty \tag{22}$$

Note that the boundary conditions for water and ether imply pure ethanol feed and are identical as long as their concentrations in the feed are the same. Conditions (21) and (22) state that the partial pressures of water and ether approach the same finite value at steady state, but not necessarily by the same path or rate. The imposition of the step change is incorporated through the velocity term, U. Greater detail in the derivation of the material balance equations is given by Yurchak (*15*) and Lehr (*10*).

TRANSIENT ADSORPTION STUDIES

To compare the mathematical model outlined here with the observed experimental results, Figures 1 and 2, it is necessary to solve simultaneously Equations (6) to (9), (13), (17) and (18). For a solution to be obtained, numerical values must be available for the reaction and adsorption rate coefficients in Equations (6) to (9). The forward and reverse rate coefficients for the surface reaction are known from the determination of Equation (10) in the steady state studies (7) and can be calculated via the relationships given here in conjunction with that equation. Experimental transient adsorption studies were required to obtain numerical values for the adsorption and desorption rate coefficients.

EXPERIMENTAL STUDIES

The transient adsorption data were obtained by Kabel (*6*) and Lehr (*10*) on similar equipment. Static adsorption systems allowing independent control of adsorption temperature and pressure were employed. A resin sample, suspended from a calibrated quartz helix, was allowed to achieve equilibrium with a vacuum (the bone dry state) or with a desired vapor pressure of adsorbate. The vapor pressure was then increased (decreased) and the transient process of adsorption (desorption) followed by observing the change in length of the helix. In this way data were obtained of moles of component adsorbed per gram of catalyst as a function of time. Runs were made at a variety of initial and final vapor pressures for water at 50, 79, 100, 116, and 120°C. and for alcohol at 79, 100, 116, and 120°C. A typical run for alcohol adsorption onto a bone dry resin at 120°C. and an exposed pressure of

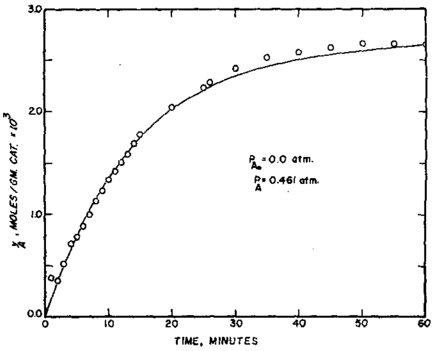

Fig. 3. Transient adsorption data for ethanol at 120°C.

0.461 atm. is illustrated in Figure 3.

TREATMENT OF DATA

To obtain an expression to represent such graphs, recourse is again made to the Langmuir theory of activated adsorption, as expressed by Equation (6) for ethanol. In recognizing that $\rho_A = dy_A/dt$, $\theta_V = 1 - \theta_A$, and $\theta_A = y_A/y_m$ one obtains the first order linear differential equation

$$\frac{dy_A}{dt} + \frac{\kappa_A P_A + \kappa_{-A}}{y_m} y_A = \kappa_A P_A \tag{23}$$

By integrating Equation (23) with the boundary condition that at $t = 0$, $y_A = y_{A_0}$, and noting that $K_A = \kappa_A/\kappa_{-A}$ one gets

$$y_A = C_1 + (y_{A_0} - C_1)\, e^{-C_2 t} \tag{24}$$

where:

$$C_1 = \frac{K_A P_A}{(1 + K_A P_A)} y_m \tag{25}$$

$$C_2 = (\kappa_A P_A + \kappa_{-A})/y_m \tag{26}$$

It will be seen that at $t = 0$, $y_A = y_{A_0}$. As t becomes large y_A approaches C_1, which is the equilibrium adsorption point for the corresponding pressure P_A. Equation (25) is really identical to Equation (6) evaluated at equilibrium. While C_1 is characteristic of equilibrium conditions, the constant C_2 relates to the magnitude of adsorption change with time.

Nonlinear regression analysis was used to fit Equation (24) to all the available transient adsorption data and to determine the constants C_1 and C_2. From these constants and Equations (25) and (26) the adsorption rate coefficients were calculated. Since the coefficients should be dependent only upon temperature, the values obtained from all runs on a given compound at a single temperature were averaged. The average of the values at 120°C. could be used directly and 105°C. coefficients could be obtained from the results at various temperatures by interpolation on an Arrhenius plot.

A complication arises in that adsorbed ethanol reacts to form adsorbed water and ethyl ether. Because the adsorption of ethanol is much more rapid than the surface reaction and because the ethanol reservoir from which adsorption occurs contains much more ethanol than the adsorbent, only a very small proportion of the adsorbate is water and ethyl ether. Thus the observed adsorption behavior really is characteristic of pure ethanol.

As can be seen from Figure 3, the fits obtained for ethanol were good. For water the calculated y vs. t curves rose somewhat less steeply than the experimental data, crossed over the experimental curve, and finally leveled out at the experimental steady state as it must. This tendency is clearly shown in Figure 4. Here the initial amount adsorbed is well above the origin. Because of the resulting small range of y_W, data scatter exaggerate somewhat this defect in the fit.

It was found in the steady state work (7) that the Langmuir isotherm had correlated well the equilibrium adsorption data for ethanol while being less satisfactory for water. This was attributed to the much greater tendency of water to adsorb in multilayers. Upon adsorption an ethanol molecule becomes a carbonium ion and a water molecule becomes a hydronium ion. Adsorption of additional water molecules on a hydronium ion would be expected to occur more easily than ethanol molecules on carbonium ions. This same explanation is believed to apply here to the nonequilibrium data.

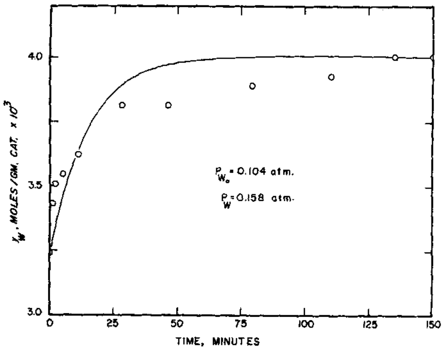

Fig. 4. Transient adsorption data for water at 120°C.

The adsorption of ethyl ether on the catalyst is sufficiently small, even at equilibrium (7), that the measurement of rates would be very difficult. For this reason and because the effects of ether adsorption will be small in comparison to those of ethanol and water it was considered adequate to estimate values for the ether adsorption rate coefficient.

PERSCRUTATION OF THE MODEL

Before proceeding to the solution of the equations it is well to consider the appropriateness of the use of Langmuir-Hinshelwood kinetics and the Langmuir adsorption isotherm. The internal consistency of the model should also be examined.

The Langmuir-Hinshelwood model of heterogeneous catalysis, as elaborated and popularized by Hougen and Watson, has achieved considerable success in empirically correlating catalytic reaction rate data. Since the Langmuir adsorption isotherm is the basis for the model, the model has been criticized on the grounds that the Langmuir theory ordinarily does not account properly for pure component adsorption without reaction. How then could it be expected to apply to multicomponent adsorption with reaction? This is a reasonable criticism. A partial answer may be attempted in a qualitative way.

When multilayer adsorption occurs, the heat of adsorption is usually much greater for the first molecule adsorbed on a given site than for succeeding molecules. Accordingly only the first molecule may be sufficiently activated to enter into the surface reaction. The Langmuir theory is restricted to monolayer adsorption and hence may be completely unsuccessful in correlating total adsorption data. Yet when applied to catalysis, where only the first layer may be active, it may achieve success by considering only the significant adsorption.

The present work is complicated by the fact that both the total adsorption and that portion of the total adsorption which is significant to the chemical reaction must be accounted for simultaneously. Kabel and Johanson (7) found approximate agreement between the Langmuir equilibrium adsorption constants determined from total adsorption measurements and those obtained from the reaction rate correlation. Thus for this particular reaction system the potential complication of inconsistency between total adsorption and activated adsorption is relived to a great extent, although not completely.

Thus the Langmuir theory is chosen for use in the model to account for both adsorption and the catalytic reaction. It would be possible to account for total adsorption by some arbitrary empirical function and for the reaction rate by the Langmuir-Hinshelwood approach, but this would involve specification of what fraction of all the adsorbed molecules were located in the first layer.

This could only be guessed and such sophistication does not seem warranted at this time.

Since the Langmuir theory is invoked at every opportunity the model becomes internally consistent. It must be recognized that where the Langmuir theory breaks down the model becomes inherently inaccurate.

Another question of internal consistency arises in the selection of adsorption rate coefficients and equilibrium constants. One constraint arises from the fact that the transient curve should coincide with the final steady state solution at large time. Equation (10) is the steady state rate equation shown to apply at 120°C. and assumed to be applicable at 105.8°C.‡ (7). The values of the adsorption equilibrium constants and forward surface reaction rate coefficients are obtained from the following equations:

At 120°C.

$$K_A = 3.413 + 4.413\, K_E \tag{27}$$

$$K_W = 0.816 + 1.816\, K_A \tag{28}$$

$$k_A = 1.369 \times 10^{-4}\, (1 + K_A)^2/K_A{}^2 \tag{29}$$

At 105.8°C.

$$K_A = 8.860 + 9.860\, K_E \tag{30}$$

$$K_W = 1.333 + 2.333\, K_A \tag{31}$$

$$k_A = .3258 \times 10^{-4}\, (1 + K_A)^2/K_A{}^2 \tag{32}$$

The basis for these equations is given elsewhere (*6*, *7*).

From Equations (27) to (32) it can be seen that once K_E is specified the remaining constants can be calculated at the same temperature. As discussed previously the obvious specification for K_E at 120°C. is zero. However since Figure 1 indicates significant adsorption of ether at 105°C., the small but finite $K_E = 0.176$ calculated by Kabel and Johanson (*7*) is selected at 120°C. for consistency. Because no data were available for determination of K_E at 105.8°C., values ranging from 0.5 to 5.0 were used in the computations. The numerical values actually used in computing the curves shown on Figures 1 and 2 are given in Table 1.

So far the selection of constants has been made from the results of steady state reaction rate data on the grounds that the transient response must satisfy the steady state case in the limiting situation. However the adorption rate coefficients must be obtained from transient adsorption experiments. Because of the restriction that $K_A = \kappa_A/\kappa_{-A}$, etc. and the fact that K_A is already specified, only one of the adsorption rate coefficients may be taken independently from the transient adsorption data via Equation (26).§ The value of κ_{-E} was estimated by similarity to the other rate coefficients and by the assumption that desorption of ethyl ether would be rapid. Further details on constant evaluation are available (*6*, *10*). The constants resulting from these procedures are shown in Table 1.

TABLE 1. SUMMARY OF KINETIC AND ADSORPTION CONSTANTS WITH MISCELLANEOUS REACTOR PARAMETERS

Quantity	105.8°C.	120°C.
K_{eq}	30.2	25.2
K_A	18.72	4.19
K_W	45.01	8.425
K_E	1.00	0.176
k_A	3.62×10^{-5}	2.10×10^{-4}
κ_A	1.20×10^{-3}	1.17×10^{-3}
κ_{-W}	2.22×10^{-4}	6.05×10^{-4}
κ_{-E}	1.00×10^{-3}	5.0×10^{-3}
y_m	5.40×10^{-3}	5.40×10^{-3}
L	5.0	18.0
A	9.05	5.06
W_c	36.92	16.774
ρ_c	0.816	0.184
P	1.0	0.956
ρ_{vA}	0.785	0.781

Parameters pertaining to reactor geometry, etc. are also given in Table 1. The value of y_m was obtained from the exchange capacity of the resin catalyst by assuming that each hydrogen ion acts as a single adsorption site.

SOLUTION OF EQUATIONS

Equation (7) accounts for the rate of reaction of ethanol and the rates of formation of ethyl and water by virtue of the stoichiometric relationship, $r_A = 2r_E = 2r_W$. When one incorporates the appropriate surface reaction rate expressions into the unsteady state material balance equations, Equations (13), (17) and (18), the following equations, rearranged and reduced to generalized notation for simplicity of manipulation, are obtained:

$$\frac{\epsilon}{U}\frac{\partial P_A}{\partial t} + \frac{\partial P_A}{\partial Z} = \frac{\rho_c RT}{U}\,[f_1(P_A,P_W,P_E,\theta_A,\theta_W,\theta_E)] \tag{33}$$

$$\frac{\epsilon}{U}\frac{\partial P_W}{\partial t} + \frac{\partial P_W}{\partial Z} = \frac{\rho_c RT}{U}\,[f_2(P_A,P_W,P_E,\theta_A,\theta_W,\theta_E)] \tag{34}$$

$$\frac{\epsilon}{U}\frac{\partial P_E}{\partial t} + \frac{\partial P_E}{\partial Z} = \frac{\rho_c RT}{U}\,[f_3(P_A,P_W,P_E,\theta_A,\theta_W,\theta_E)] \tag{35}$$

There are now three equations with six dependent variables. Since $\rho_A' = y_m\, (\partial\theta_A/\partial t)_Z$ etc., and $\theta_V = 1 - \theta_A - \theta_W - \theta_E$ Equations (6), (8) and (9) may be written in the functional form

$$\frac{\partial\theta_A}{\partial t} = f_4\,(P_A,\theta_A,\theta_W,\theta_E) \tag{36}$$

$$\frac{\partial\theta_W}{\partial t} = f_5\,(P_W,\theta_A,\theta_W,\theta_E) \tag{37}$$

$$\frac{\partial\theta_E}{\partial t} = f_6\,(P_E,\theta_A,\theta_W,\theta_E) \tag{38}$$

In effect three more equations have been added without increasing the number of dependent variables. All six equations must be solved simultaneously. In addition to the initial conditions given by Equations (14), (15), (19), and (20) the initial fractional surface coverage of all components at all points in the reactor is required. These can be calculated from equations corresponding to the following one for alcohol:

$$\theta_A = K_A P_A/(1 + K_A P_A + K_W P_W + K_E P_E) \tag{39}$$

For θ_E and θ_W, $K_A P_A$ in the numerator is replaced by $K_E P_E$ and $K_W P_W$, respectively.

METHOD OF CHARACTERISTICS

The simultaneous solution of Equations (33) to (38) would be considerably more complex and time consuming were it not for the method of characteristics. Acrivos (*1*) has described this technique and provided examples of

---

‡ There is a small discrepancy between the temperature of the transient run (105°C.) and the temperature of the corresponding steady state kinetic studies (105.8°C.). It is so small as to have no appreciable effect on the results of this paper.

§ The fact that the adsorption rate coefficient for ethanol, κ_A, has essentially the same magnitude at 105.8°C. as at 120°C. results from the inconsistency between the temperature dependencies of κ_{-A} determined in transient adsorption studies of K_A obtained from the steady state kinetic studies.

its use in problems of fixed bed adsorption and other areas of interest to chemical engineers. The method is applicable to any set of totally hyperbolic partial differential equations, a criterion met in this case.

For this problem the method of characteristics requires that integration be performed along lines in the space-time domain defined by

$$\frac{dZ}{dt} = U_i = \frac{U}{\epsilon} \tag{40}$$

To find the equivalent of Equation (33) the total derivative of P_A is written

$$\frac{dP_A}{dZ} = \frac{\partial P_A}{\partial t}\left(\frac{dt}{dZ}\right) + \frac{\partial P_A}{\partial Z} \tag{41}$$

As discussed earlier the approximation is made that the velocity is indpendent of position in the reactor throughout the transient period. The method of characteristics also applies to the case where velocity varies with distance through the reactor and with time, but the additional complexity is not warranted in this case. Equation (41) may now be rewritten

$$\frac{dP_A}{dZ} = \frac{\epsilon}{U}\frac{\partial P_A}{\partial t} + \frac{\partial P_A}{\partial Z} \tag{42}$$

With Equation (42), Equation (33) may be reduced to an ordinary differential equation by integrating along the characteristic defined by $dZ/dt = U_i$. This characteristic is denoted as *characteristic I.*

Thus

$$\left(\frac{dP_A}{dZ}\right)_I = \frac{\rho_c RT}{U}\left[f_1\left(P_A,P_W,P_E,\theta_A,\theta_W,\theta_E\right)\right] \tag{43}$$

By analogy,

$$\left(\frac{dP_W}{dZ}\right)_I = \frac{\rho_c RT}{U}\left[f_2\left(P_A,P_W,P_E,\theta_A,\theta_W,\theta_E\right)\right] \tag{44}$$

$$\left(\frac{dP_E}{dZ}\right)_I = \frac{\rho_c RT}{U}\left[f_3\left(P_A,P_W,P_E,\theta_A,\theta_W,\theta_E\right)\right] \tag{45}$$

Equations (36) to (38) were written as partial derivatives with respect to time at constant Z. Thus they too may be treated as ordinary differential equations if they are integrated along the time dimension at a given reactor position. With the time coordinate designated *characteristic II* the following equations arise:

$$\left(\frac{d\theta_A}{dt}\right)_{II} = f_4\left(P_A,\theta_A,\theta_W,\theta_E\right) \tag{46}$$

$$\left(\frac{d\theta_W}{dt}\right)_{II} = f_5\left(P_W,\theta_A,\theta_W,\theta_E\right) \tag{47}$$

$$\left(\frac{d\theta_E}{dt}\right)_{II} = f_6\left(P_E,\theta_A,\theta_W,\theta_E\right) \tag{48}$$

DESCRIPTION OF COMPUTATIONS

A third-order Runge-Kutta numerical integration method (*2*) was used to integrate Equations (43) to (45) along characteristic I simultaneously with the integration of Equations (46) to (48) along characteristic II. Equation (46) can be integrated analytically for θ_A as a function of time by taking θ_E and θ_W to be constant at a mean value over the increment of time. θ_W is obtained by taking θ_A and θ_E constant; θ_E is obtained by taking θ_A and θ_W constant. The equations are solved simultaneously with each set of newly calculated values used to obtain new mean value estimates for θ_A, θ_W, and θ_E. This process is repeated until no significant changes in the calculated θ_A, θ_W, and θ_E occur. The convergence to a solution is rapid. Since the increment of time is small the approximation of constant θ's and analytical integration is justified and results in a saving of time.

A DAFT¶ Fortran computer program was written for the numerical integration of the mathematical model equations. The input to the program consisted of the values of the parameters presented in Table 1, increments at which the steps of the integration were to be carried out, and tolerances to stop iterative calculations and to specify when the new steady state had been reached initial steady state flow rate was introduced for the calculation of the initial distribution of concentrations throughout the reactor. The final flow rate specified the new gas velocity, thus determining the slope of characteristic I.

DISCUSSION OF RESULTS

Comparison of Prediction with Experiment

Graphical comparisons between predicted and experimental transient behavior are given in Figures 1 and 2. The predicted curves at both temperatures exhibit all of the qualitative characteristics of the experimental curves as discussed earlier.

Consider first the 120°C. data of Figure 2. At the initial steady state the predicted partial pressures deviate from the experimental values by 7%; at the final steady state the deviation is 5%. Since these comparisons are made between integral conversion data obtained by Lehr (*10*) and corresponding values predicted with the rate equation of Kabel and Johanson (*7*), the agreement is well within the potential error of such a comparison.

The predicted ether curve agrees excellently with the experimental data over the entire transient period. Since ethyl ether was assumed to be slightly adsorbed, a delayed minimum in ether concentration is evident in this Figure. For comparison, the instantaneous minimum that is calculated if ether is assumed to be not adsorbed is also shown. Once the postulated excess adsorbed ether has desorbed the two predicted curves become identical. The agreement between the experimental and predicted ether behavior is taken as an indication that the model has correctly accounted for the rate of reaction during the transient state. The predicted water curve falls off more rapidly and maintains a generally lower level (except in the approach to steady state) than the experimental curve. This effect is believed to be due to the inherent difficulty of accounting for total adsorption and adsorption significant to the surface reaction at the same time. Because this model does not account for adsorption of water beyond the monolayer, it predicts less water in the system both on the surface at all times and in the vapor during the transient state.

Experimental data on the simultaneous adsorption of water and ethanol on this ion exchange resin catalyst at the concentrations of interest could be used to test this hypothesis directly. Unfortunately such data are not presently available. Some feeling for the amount of water actually present on the catalyst at the initial and final conditions can be obtained from pure component adsorption data. At the existing partial pressures of water, the corresponding amounts adsorbed from pure water vapor at equilibrium can be obtained. The reductive effect of the competitive adsorption of ethanol on the amount of adsorbed water must be allowed for. After such an al-

---

¶ DAFT is a modification of Fortran II written by the Computer Science Center at The Pennsylvania State University.

lowance the estimated amount of water which must be desorbed in going from the initial to the final steady state is sixty percent greater than accounted for by the Langmuir model as used in this study.

At 105°C. much greater disagreement is seen between experimental and predicted concentrations at the initial and final steady states. The data shown on Figure 1 were obtained by Kabel (6) in a preliminary portion of his experimental program. At that time the accuracy of his results was inferior to his later work. The inaccuracies resulted from lack of refinement in experimental technique and a crude gas chromatographic calibration. On the other hand, the data upon which the 105.8°C. rate equation used in this work was based were obtained later in Kabel's experimental program and are much more reliable. In fact these integral data at the same steady state conditions used in the 105°C. transient run agree very well with the predicted initial and final concentrations.

Nevertheless inspection of predicted and experimental results for this case is illuminating. Comparison of the water curves of Figure 1 shows the same relationship as at 120°C. and the same explanation is believed to apply. The predicted ether curve has its minimum displaced from zero time as does the experimental curve, although the displacement is not so great. The displacement has been attributed earlier to significant adsorption of ether. It should be noted that beyond sixty minutes the predicted and experimental ether curves are almost exactly parallel. Thus if the final steady state inconsistency were removed by translating the experimental data vertically[#], the two ether curves would be essentially superimposed except for the early portion. Also the water curves appear in better perspective. The difference between the predicted and experimental ether curves can then be explained by presuming the effect of the minimum surface reaction rate to be masked to a greater extent than predicted by the model. For ether, the constants K_E and κ_{-E} at 105.8°C. were estimated. The magnitudes chosen seem reasonable in the light of available information, but empirical adjustment of the values would be expected to alter the shape of the predicted curve somewhat.

At both temperatures excellent agreement between experiment and prediction is obtained for the time required to reach steady state. This is taken as another indication that the rates of the surface processes have been properly accounted for. Regardless of the transient composition behavior, the capability of predicting the time to reach a new steady state has definite implications in process control work.

Consequences of the Study

This study has demonstrated that ethyl ether is significantly adsorbed at 105°C., contrary to the unverified assumption of Kabel and Johanson (7). This will lead to higher kinetically obtained equilibrium adsorption constants for ethanol and water as shown in Table 1. Thus the agreement between the equilibrium adsorption constants determined by kinetics and by adsorption will be lessened.

The model has been shown to account well for the rate processes in this heterogeneous catalytic reaction system despite its failure to properly account for total adsorption. This appears to support the idea that Langmuir-Hinshelwood model considers only the adsorption of significance in the catalytic reaction.

CONCLUSIONS

A mathematical model based on the Langmuir theory of activated adsorption and the Langmuir-Hinshelwood model of heterogeneous catalysis has been developed for the prediction of the transient behavior of a catalytic reaction system in which significant adsorption occurs. The model has been experimentally evaluated for the case of a step increase in flow rate.

The model was shown to be in qualitative agreement with all experimental observations. It accurately predicted the time required to reach a new steady state for two very different sets of conditions. The model will account for total adsorption only when multilayer adsorption does not occur.

This study has added a new dimension to the description of chemical reactors in the transient state. It has shown that investigation under unsteady state conditions can lead to a better understanding of catalytic reaction systems.

ACKNOWLEDGMENT

The authors wish to acknowledge financial support received from the E. I. duPont deNemours and Company, Inc. and the National Science Foundation for portions of this work.

NOTATION

A = cross sectional area of empty reactor, sq. cm.
C_1, C_2 = empirical curve fitted constants
$f_1, f_2, \ldots, f_n$ = arbitrary functions for adsorption and reaction rates
$f(Z)$ = initial partial pressure distribution of ethanol as a function of reactor length, atm.
$g(Z)$ = initial partial pressure distribution of water and ether as a function of reactor length, atm.
k_A = forward surface reaction rate coefficient, moles/min. g. cat.
k_{-A} = reverse surface reaction rate coefficient, moles/min. g. cat. atm.
K = surface reaction equilibrium constant, dimensionless
K_A, K_W, K_E = Langmuir equilibrium adsorption constants for ethanol, water, and ether, respectively, atm.$^{-1}$
K_{eq} = thermodynamic equilibrium constant = $K_A{}^2K/K_WK_E$, dimensionless
L = total length of packed section of reactor, cm.
M, N = arbitrary constants specifying convergence of model solution to a new steady state, atm.
P = total pressure, atm.
P_A, P_W, P_E = partial pressure of ethanol, water, and ether, respectively, atm.
r_A = rate of disappearance of ethanol, moles/min. g. cat.
r_W, r_E = rate of formation of water and ether, respectively, moles/min. g. catalyst
R = gas constant, consistent units
s = a catalytic site
t = time, min.
T = temperature, °K.
U = superficial gas velocity, cm./min.
U_i = interstitial gas velocity = U/ϵ, cm./min.
v_{Ao} = initial liquid ethanol flow rate, cc./min.
v_A = liquid ethanol flow rate, cc./min.
W_c = total weight of catalyst in reactor, g.
y_{Ao} = initial amount of ethanol adsorbed on catalyst, moles/g. catalyst
y_A = amount of ethanol adsorbed on catalyst, moles/g. catalyst

---

[#] This translation will increase the inconsistency at the initial steady state. However at that point the flow rate was so low that measurement was almost impossible. Thus the actual liquid flow rate could easily have been 0.04 cc./min. At that flow rate the predicted ether and water partial pressures would agree more closely with the adjusted experimental value.

y_m = amount of adsorbate which may be adsorbed in a monolayer on catalyst surface, moles/g. catalyst
Z = distance along reactor length, cm.

Greek Letters

δ = increase in the total number of moles in the system per mole of substance A reacted $= [(r + s + \ldots) - (a + b + \ldots)]/a$ for reaction $aA + bB + \ldots = rR + sS + \ldots$
ϵ = void fraction of packed section of the reactor, dimensionless
$\theta_A,\theta_W,\theta_E$ = fraction of catalyst monolayer covered with ethanol, water, and ether, respectively, dimensionless
θ_V = fraction of vacant catalyst sites in monolayer, dimensionless
$\kappa_A,\kappa_W,\kappa_E$ = adsorption rate coefficients for ethanol, water, and ether, respectively, moles/min. g. cat. atm.
$\kappa_{-A},\kappa_{-W},\kappa_{-E}$ = desorption rate coefficients for ethanol, water, and ether, respectively, moles/min. g. cat.
ρ_A,ρ_W,ρ_E = rate of adsorption of ethanol, water, and ether, respectively, moles/min. g. cat.
ρ_c = bulk catalyst density, g. cat./cc. reactor
ρ_M = molar density $= P/RT$, moles/cc.
ρ_{vA} = density of liquid ethanol feed, g./cc.

LITERATURE CITED

1. Acrivos, Andreas, *Ind. Eng. Chem.*, **48**, 703 (1956).
2. Arden, B. W., "An Introduction to Digital Computing," pp. 274-283, Addison Wesley, Reading, Massachusetts (1963).
3. Beek, John, "Advances in Chemical Engineering," Vol. 3, Academic Press, New York (1962).
4. Crider, J. E., and A. S. Foss, *AIChE J.*, **12**, 514 (1966).
5. Foss, A. S., *Chem. Eng. Prog. Symp. Ser. No. 25*, **55**, 47 (1959).
6. Kabel, R. L., Ph.D. thesis, Univ. Washington, Seattle, (1961).
7. ———, and L. N. Johanson, *AIChE J.*, **8**, 621 (1962).
8. ————, *J. Chem. Eng. Data*, **6**, 496 (1961).
9. Lapidus, Leon, *Chem. Eng. Prog. Symp. Ser. No. 36*, **57**, 34 (1961).
10. Lehr, C. G., MS thesis, Pennsylvania State Univ., University Park (1966).
11. McGuire, M. L., and Leon Lapidus, *AIChE J.*, **11**, 85 (1965).
12. Mullarkey, T. B., MS thesis, Pennsylvania State Univ., University Park, in progress.
13. Wilhelm, R. H., *Pure Appl. Chem.*, **5**, 403 (1962).
14. Yamas, J. L., B.S. thesis, Pennsylvania State Univ., University Park (1964).
15. Yurchak, Sergei, B.S. thesis, ibid. (1964).

Manuscript received January 26, 1967; revision received October 26, 1967; paper accepted October 27, 1967. Paper presented at AIChE Houston meeting.

Stability of Adiabatic Packed Bed Reactors:

Effect of flow variations and coupling between the particles.

JOHN W. VANDERVEEN, DAN LUSS, and NEAL R. AMUNDSON

University of Minnesota, Minneapolis, Minnesota

A simple cell model is used for the determination of necessary and sufficient conditions for the stability of an adiabatic fixed bed reactor. These conditions are stronger than those obtained by considering only a perturbation of a single particle. Because of the nonuniqueness of the steady state profiles certain pathological effects can occur when the flow rate of the reactant is changed. Geometric coupling between the particles and heat transfer by radiation give rise to further complexities. Examples are given in which the trends predicted by the models have been observed experimentally by Wicke and Frank-Kamenetskii.

In the last decade a great deal of effort has been expended in an attempt to characterize the behavior of fixed bed reactors. This problem is of practical importance since an increasing number of industrially important reactions are carried out in fixed and moving beds, and a number of papers dealing with both theoretical and experimental results have appeared.

This study is based on earlier work (5) in which a simple continuous model of an adiabatic reactor with the reaction $A \rightarrow B$ showed the significance of the transient behavior of the bed. It was demonstrated that each catalyst pellet could, under suitable conditions, exist in

---

John W. Vanderveen is with Phillips Petroleum Company, Bartlesville, Oklahoma, and Dan Luss is at the University of Houston, Houston, Texas.